Capacity Modeling and Routing for Traffic Networks with Mixed Autonomy

Daniel A. Lazar[1], Samuel Coogan[2] and Ramtin Pedarsani[3]

***Abstract*— Transportation infrastructure is entering a stage of mixed use whereby vehicles are capable of varying levels of autonomy, and investigating the potential benefits of this mixed infrastructure is a critical step to fully realizing the mobility benefits of autonomy. In this paper, we consider a mixed traffic profile where a fraction of vehicles are smart and able to form platoons, and the remaining are regular and manually driven. We develop two models for road capacity under mixed autonomy that are based on the fundamental behavior of autonomous technologies such as adaptive cruise control. Moreover, we formulate an optimal routing problem of mixed traffic for the first capacity model with two parallel roads. We first study the case that a planner aims to minimize the social cost of the system, and has control over both regular and smart traffic flows. We prove that this optimization problem is convex for the chosen road delay function, and fully characterize its optimal solution. We further study the case that only smart vehicles can be controlled and the regular vehicles choose their route selfishly according to the best response to the routing choice of smart vehicles. Finally, we provide extensive numerical studies that corroborate our analytical results.**

I. INTRODUCTION

In the coming years and decades, vehicles equipped with autonomous capabilities will become increasingly prevalent, providing new opportunities to improve mobility and traffic flow. For example, cooperative platooning has the potential to smooth traffic flow and increase highway capacity [1], [2], and platoons of connected vehicles can more than double throughput in urban roads [3].

However, fully autonomous vehicles will not become ubiquitous overnight and vehicles with varying levels of autonomy will coexist with manually driven vehicles into the foreseeable future. Indeed, semiautonomous technology such as adaptive cruise control (ACC) and automated lane-keeping are already available on many passenger vehicles. Such features are currently designed and marketed for the convenience of the driver, but their growing availability and popularity demands new research into how these emerging technologies affect network-level mobility, especially as vehicles equipped with this technology will continue to interact with conventional, nonautonomous vehicles.

On freeways, when all vehicles are equipped with the requisite automation features, significant improvement can be achieved [4], [5], [6]. Simulation studies suggest that low penetration rates of semiautonomous vehicles do not lead to considerable improvement while higher levels of penetration can lead to significant increases in traffic throughput [7], [8], [9], [10], [11], [12].

At signalized intersections, much of the literature has focused on using autonomy to schedule vehicle crossings at an intersection with the goal of achieving signal-less intersection control; see, *e.g.*, [13], [14], [15], [16], [17], [18] and references therein. In that case, all vehicles must be equipped with autonomous control and communication capabilities and thus implementation of such strategies likely remains years or decades away. The recent paper [19] appears to be the first to study the impact of mixed autonomy at signalized intersections using various car-following models in a microsimulation environment.

In this paper, we propose a model for road capacity derived from the principle that vehicles with autonomous capabilities are able to maintain shorter headways to preceding vehicles. The road capacity is then a function of the fraction of vehicles with autonomous capabilities. Next, we consider the case when vehicle routes can be altered in order to adjust the fraction of vehicles with autonomous capabilities on each road. We solve this problem in the case of two parallel roads when a social planner aims at minimizing the social cost of the system, and has control over both vehicle types. We then study the case when vehicles with autonomous capabilities can be prescribed a particular route for societal gain, while the remaining vehicles behave selfishly. While this problem proves to be far more challenging, we present computation and simulation results which suggests that it is convex.

We assume the network will achieve a Wardrop or user equilibrium [20], [21], [22], [23] whereby drivers choose routes that they perceive as being the shortest under the prevailing traffic conditions. As user equilibria typically do not minimize the social cost, Koutsoupias and Papadimitriou proposed to analyze the inefficiency of equilibria from a worst-case perspective, and introduced the notion of "price of anarchy" [24], [25], which is the ratio of the worst social cost of a Wardrop equilibrium to the cost of an optimal solution. In [26], the authors showed that the price of anarchy is bounded for a certain class of cost functions. Similar results were obtained for more general network models in [27], [28], [29], [30]. In this paper, we establish initial results that extend some of these ideas to the mixed autonomy setting with autonomy-dependent capacities and costs.

The rest of the paper is organized as follows. We present two capacity models for roads with mixed autonomy in

[1]Daniel Lazar is with the Department of Electrical and Computer Engineering, University of California, Santa Barbara dlazar@ece.ucsb.edu

[2]Samuel Coogan is with the School of Electrical and Computer Engineering and the School of Civil and Environmental Engineering, Georgia Institute of Technology sam.coogan@gatech.edu

[3]Ramtin Pedarsani is with the Department of Electrical and Computer Engineering, University of California, Santa Barbara ramtin@ece.ucsb.edu

Section II, followed by a full description of social planner and selfish routing optimization problems in Section III. We discuss numerical results in Section V and conclude the paper in Section VI.

II. Modeling Mixed Autonomy

The Highway Capacity Manual defines the capacity of a road as the maximum possible flow rate on the road in vehicles per hour [31]. Capacity is primarily limited by the average headway that vehicles maintain while traveling on the road, and the HCM recommends a nominal saturation flow rate of 1900 vehicles per hour (vph) per lane to capture typical behavior of drivers, which corresponds to a headway of $3600/1900 = 1.89$ seconds (s).

With the emergence of semiautonomous driving technology such as cooperative adaptive cruise control (CACC), it is projected that the headway can be reduced to approximately 0.8 s, which corresponds to a road capacity of 4500 vph [32]. However, to achieve this nearly 2.5-fold increase in capacity requires every vehicle to maintain shorter headways. What happens when only a fraction of vehicles are equipped with the required technology to achieve reduced headway? In this section, we consider two possible models for reduced headways and increased capacity in this *mixed autonomy* setting. We say a vehicle is *smart* if it is equipped with semiautonomous driving capabilities that enable reduced headways, and *regular* otherwise.

A. Capacity Model 1

We first consider a scenario in which each smart vehicle is able to maintain reduced headway with any preceding vehicle, regardless of whether that vehicle is also equipped with driver assistance technology. This scenario is plausible when smart vehicles are able to accurately localize any surrounding vehicle without communication. At the moment, it is unclear whether a sufficiently sophisticated sensor suite for this task will be omnipresent on autonomous vehicles. Indeed, the sensors likely required to achieve this feat, such as lidar, are currently prohibitively expensive for mass adoption. On the other hand, companies such as Tesla have focused on enabling autonomous technology by relying primarily on cameras [33].

Suppose that m is the capacity of the road when fully utilized by regular vehicles, and M is the capacity when fully utilized by smart vehicles, where $M > m$. Let α be the *average* fraction of smart vehicles on the road. We call α the *autonomy level* of the road. Define $C(\alpha)$ to be the capacity of the road under autonomy level α. We propose the following approximation:

$$C(\alpha) = (\alpha M^{-1} + (1-\alpha)m^{-1})^{-1}. \tag{1}$$

Here is a justification for (1). First, assume that every smart vehicle follows the preceding vehicle (whether it is smart or regular) with time gap of $t_2 = M^{-1}$. Second, assume that each regular vehicle follows the preceding vehicle with time gap of $t_1 = m^{-1}$ where $t_1 > t_2$. Finally, since a fraction α of vehicles are smart, the effective headway of the road with autonomy level α is $\alpha t_2 + (1-\alpha)t_1$, which implies (1). Note that this approximation is valid regardless of how the smart vehicles are distributed among the regular vehicles, so long as the autonomy level is α.

In Figure 1, we plot road capacity as a function of the fraction of smart vehicles α, assuming that the capacity when there are no smart vehicles ($\alpha = 0$) is 1900 vph and when there are only smart vehicles ($\alpha = 1$) is 4500 vph.

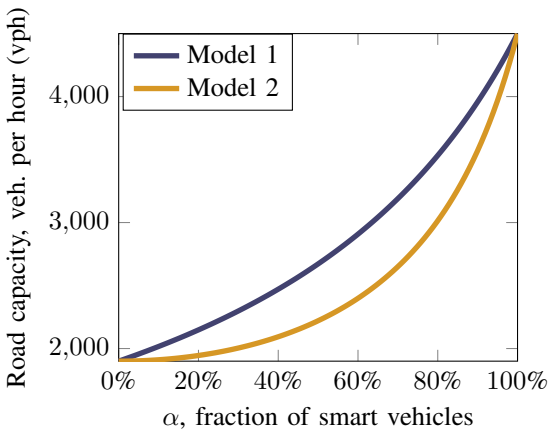

Fig. 1: Road capacity as a function of the autonomy level α, *i.e.*, the ratio of smart vehicles on the road. In Model 1 (dark/blue), it is assumed that smart vehicles are able to maintain shorter headways with any preceding vehicle. In Model 2 (light/orange), it is assumed that smart vehicles are only able to maintain a shorter headway if the preceding vehicle is also smart, with results in decreased capacity.

B. Capacity Model 2

We now consider an alternative model in which a smart vehicle is only able to maintain a short headway if the preceding vehicle is also smart. As above, suppose that m (respectively, M) is the capacity of the road when fully utilized by regular (respectively, smart) vehicles, and again let α be the average fraction of smart vehicles on the road.

Unlike the previous model, the capacity of the road now depends on the distribution of smart vehicles among regular vehicles. For example, consider a single-lane road with n vehicles, and suppose $n/2$ are regular and $n/2$ are smart. In the extreme case that the smart and regular vehicles are perfectly interleaved such that every smart vehicle is preceded by a regular one, then the capacity is m and no gain is achieved. In the other extreme case that a platoon of $n/2$ smart vehicles precedes $n/2$ regular vehicles, the throughput of the road becomes the same as (1). Therefore, a proper definition of the capacity of the road depends on the *stochastic process* of the vehicles traversing the road.

Here, we propose to model vehicle type as a Bernoulli process, *i.e.*, each vehicle is smart with probability α and regular with probability $1-\alpha$ independently. In this case, the capacity of the road is approximated as

$$C(\alpha) = (\alpha^2 M^{-1} + (1-\alpha^2)m^{-1})^{-1}. \tag{2}$$

To derive (2), note that the time gap between two vehicles is $t_2 = M^{-1}$ if they are both smart and $t_1 = m^{-1}$ otherwise. Thus, one needs to count the fraction of pairs of smart

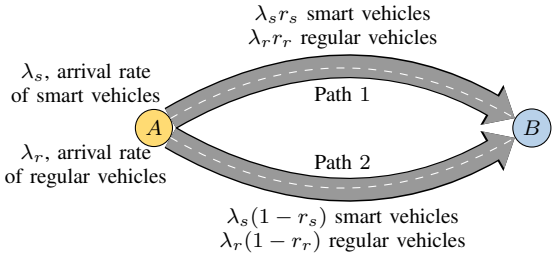

Fig. 2: Diagram of the routing problem, with regular and smart cars arriving at node A and taking path 1 or path 2 to node B. Section III develops delay models for each road and a social cost function for this configuration.

vehicles, which is α^2. This implies that the average headway is $\alpha^2 t_2 + (1-\alpha^2)t_1$. Figure 1 also plots the capacity model (2).

III. Routing Problem Formulation

In this section we develop a congestion model and social cost function for mixed traffic on two parallel roads and describe the optimization problem in which a social planner controls all vehicles. We present Theorem 1 that establishes the convexity of this optimization problem and the location of its minimum, which follow from a geometric interpretation of the cost function. We finish this section by formulating the problem in which regular cars choose their routes selfishly.

A. Model Description, Capacity Model 1

In this subsection we present our model for the social cost of traffic in the network using capacity model 1 (1). The fundamental diagram of traffic and the M/M/1 queuing model motivate the delay model, which describes a negative linear relationship between service speed and arrival rate.

In our model, we consider arrival rates of λ_r regular vehicles and λ_s smart vehicles per hour that will travel over path 1 or path 2 as illustrated in Fig. 2. The portion of regular and smart vehicles to travel on road 1 are denoted by r_r and r_s, respectively, for the region of consideration $r_r, r_s \in [0,1]$. This corresponds to a regular (respectively smart) flow of $\lambda_r r_r$ ($\lambda_s r_s$) vehicles per hour on road 1 and $\lambda_r \overline{r}_r$ ($\lambda_s \overline{r}_s$) vehicles per hour on road 2.

The autonomy level, the unitless measures of the fraction of vehicles on a road that are smart, of the roads are

$$\alpha_1(r_r, r_s) = \frac{\lambda_s r_s}{\lambda_r r_r + \lambda_s r_s}\ ;$$
$$\alpha_2(\overline{r}_r, \overline{r}_s) = \frac{\lambda_s \overline{r}_s}{\lambda_r \overline{r}_r + \lambda_s \overline{r}_s} = \frac{\lambda_s(1-r_s)}{\lambda_r(1-r_r) + \lambda_s(1-r_s)}\ .$$

The capacity of each road is a function of the autonomy level of the road, with parameters M and m (described in Section II-A). The flow capacity terms below, with unit vehicles per hour, represent the maximum arriving *mixed* flow that can be served by the road. Using a and c to denote the regular capacity of roads 1 and 2 respectively and b and d to denote the smart capacity of roads 1 and 2, the mixed road capacities are $C_1(\alpha_1) = \frac{ab}{\alpha_1 a + (1-\alpha_1)b}$ and $C_2(\alpha_2) = \frac{cd}{\alpha_2 c + (1-\alpha_2)d}$.

Considering a negative linear relationship between service speed and arrival rate, we express the delay function (with unit hours per vehicle) associated with each road as

$$D_1(r_r, r_s, C_1) = \frac{1}{C_1 - (\lambda_r r_r + \lambda_s r_s)}\ ;$$
$$D_2(\overline{r}_r, \overline{r}_s, C_2) = \frac{k}{C_2 - (\lambda_r \overline{r}_r + \lambda_s \overline{r}_s)} \tag{3}$$

where k is a scalar denoting the length difference between the two roads, with unit kilometers per kilometers. This assumes that the congestion on each road is uniform on its length.

The cost function represents the social cost, or aggregate delay, associated with the congestion:

$$\begin{aligned} L(r_s, r_r) &= (\lambda_r r_r + \lambda_s r_s) D_1 + (\lambda_r \overline{r}_r + \lambda_s \overline{r}_s) D_2 \\ &= \frac{b\lambda_r r_r + a\lambda_s r_s}{ab - b\lambda_r r_r - a\lambda_s r_s} + \frac{k(d\lambda_r \overline{r}_r + c\lambda_s \overline{r}_s)}{cd - d\lambda_r \overline{r}_r - c\lambda_s \overline{r}_s}\ . \end{aligned} \tag{4}$$

The cost function is unitless, and denotes the total amount of delay experienced by the vehicles in the system in 1 hour.

B. Social Planner Optimization

In this subsection we present an optimization problem where a social planner aims at minimizing the system's cost function. In social planner optimization we assume control over the flows of both types of traffic, i.e. r_r and r_s. Then, the optimization problem is as follows:

$$\begin{aligned} (r_s^{OPT}, r_r^{OPT}) = &\operatorname*{argmin}_{r_s, r_r} L(r_s, r_r) \\ s.t. \quad & r_s, r_r \in [0,1],\ ab > b\lambda_r r_r + a\lambda_s r_s, \\ & cd > d\lambda_r \overline{r}_r + c\lambda_s \overline{r}_s\ . \end{aligned} \tag{5}$$

The delay functions D_1 and D_2, which grow to infinity as the flows approach road capacity, bound the feasibility region of r_r and r_s. This feasibility region is dictated by the latter two constraints in (5) and is shown in the unshaded portion of Fig. 3. The upper and lower lines represent the constraints imposed by the capacities of road 1 and 2, respectively. If the constraint line for road 2 is entirely above the line for road 1 in the region of consideration, $r_r, r_s \in [0,1]$, then no flow configuration can result in a finite user delay time.

In addition to showing the feasibility region, Fig. 3 sets up a geometric interpretation of the cost function that makes explicit the dependence of the cost function on the distance from the point considered to the lines bounding the feasibility region. The distance between $(\hat{r}_s, \hat{r}_r)$ and the lines describing the constraint imposed by roads 1 and 2 is denoted by h_1 and h_3, respectively. The constants h_2 and h_4 depend on the distance of the constraint lines from the origin and the point $(1,1)$[1]. The cost then becomes

$$L(r_s, r_r) = L_g(h_1, h_3) = \frac{h_2 - h_1}{h_1} + k\frac{h_4 - h_3}{h_3}\ . \tag{6}$$

[1]The locations of the intersections of the feasibility lines with the axes in Fig. 3 are still valid outside the region of consideration, and the definitions of h_1, h_2, h_3, and h_4 are independent of the specific example shown in the figure. Therefore the equality between (4) and (6) is valid whether or not the feasibility lines are within the region of consideration.

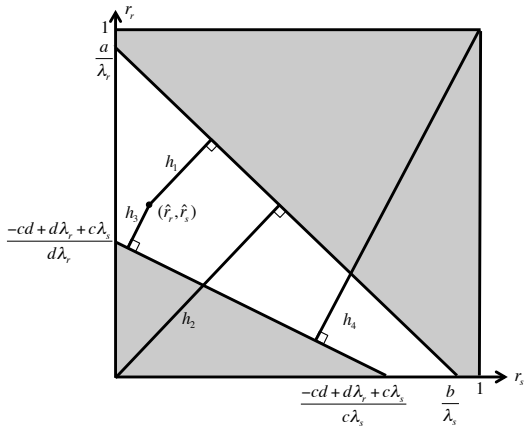

Fig. 3: Geometric representation of the cost function. The unshaded portion is the set of feasible traffic configurations. The cost associated with routing ($\hat{r}_s$,$\hat{r}_r$) is a function of the distance of the point to the feasibility lines. This structure implies convexity and limits social optimal solutions to the extremity of the region of consideration ($r_r, r_s \in [0,1]$).

To show the equality between (4) and (6), we investigate the area of four triangles in Fig. 3:

(1) $A_1 = \frac{h_1 b_1}{2}$, the area of the triangle formed by the points $(0, \frac{a}{\lambda_r})$, $(\frac{b}{\lambda_s}, 0)$, and $(\hat{r}_s, \hat{r}_r)$,

(2) $A_2 = \frac{h_2 b_1}{2}$, the area of the triangle formed by the points $(0, \frac{a}{\lambda_r})$, $(\frac{b}{\lambda_s}, 0)$, and $(0,0)$,

(3) $A_3 = \frac{h_3 b_2}{2}$, the area of the triangle formed by the points $(0, \frac{-cd+d\lambda_r+c\lambda_s}{d\lambda_r})$, $(\frac{-cd+d\lambda_r+c\lambda_s}{c\lambda_s}, 0)$, and $(\hat{r}_s, \hat{r}_r)$, and

(4) $A_4 = \frac{h_4 b_2}{2}$, the area of the triangle formed by the points $(0, \frac{-cd+d\lambda_r+c\lambda_s}{d\lambda_r})$, $(\frac{-cd+d\lambda_r+c\lambda_s}{c\lambda_s}, 0)$, and $(1,1)$.

Above, b_1 and b_2 are the lengths of the feasibility lines for roads 1 and 2, respectively, in the region of consideration. We then see that $L(r_s, r_r) = \frac{A_2 - A_1}{A_1} + k\frac{A_4 - A_3}{A_3} = L_g(h_1, h_3)$.

Finding the optimal routing then becomes

$$\begin{aligned}(h_1^{OPT}, h_3^{OPT}) = &\operatorname*{argmin}_{h_1,h_3} L(h_1, h_3)\\ &\text{s.t.} \quad \text{region of consideration,}\\ &\qquad \text{feasibility constraints.}\end{aligned} \tag{7}$$

With this in mind, we present the following theorem:

Theorem 1: Assuming the intersection of the feasibility region and the region of consideration is nonempty, (5) is convex and the minimum of the cost function occurs at an extremity (*i.e.* $r_s = 0$, $r_r = 0$, $r_s = 1$, or $r_r = 1$) of the region of consideration, $r_s, r_r \in [0,1]$.

Proof: Consider $L_g(h_1, h_3)$ as the sum of two functions, $\frac{h_2}{h_1} - 1 + \frac{kh_4}{h_3} - k = f(h_1) + g(h_3)$. Here $f(h_1)$ and $g(h_3)$ are convex in h_1 and h_3, for all h_2, h_4, and $k > 0$. Since the sum of two convex functions is convex, L_g is convex.

The second part uses a geometric argument motivated by monotonicity in the cost function. Consider two cases:

1) $\frac{a}{b} \neq \frac{c}{d}$: Assume the optimal routing point within the feasibility region, with cost $L^{OPT} = L_g(h_1^{OPT}, h_3^{OPT})$, is in the interior of the region of consideration. Since $\frac{a}{b} \neq \frac{c}{d}$, there exists a point for which $h_1 = h_1^{OPT}$ and $h_3 > h_3^{OPT}$. For a constant h_1, the cost function is inversely proportional to h_3 so the cost monotonically decreases as h_1 is fixed and h_3 increases, and $L(h_3, h_1^{OPT}) < L^{OPT}$. This contradicts the premise that L^{OPT} achieves the minimum cost in the interior of the feasible region of consideration.

2) $\frac{a}{b} = \frac{c}{d}$: Assume the optimal routing point is in the interior of the feasibility region, with cost $L^{OPT} = L_g(h_1^{OPT}, h_3^{OPT})$. Since the feasibility lines are parallel, the minimum is not unique and there exists a line for which $h_1 = h_1^{OPT}$ and $h_3 = h_3^{OPT}$ where every point on that line is a minimizer of the cost function. That line intersects with the r_s-axis and r_r-axis, so there is an extreme point of the feasibility region with the same cost.

■

This theorem will be used in Section IV to develop a closed-form solution for the social planner optimization.

C. Selfish Routing for Regular Vehicles

In the previous subsection we considered the case in which a social planner chooses routes for both regular and smart vehicles. Here we consider the more realistic case in which regular vehicles choose their own routes to minimize their individual delays.

When the operators of the regular vehicles choose their routes we assume that they will do so selfishly, thereby choosing the road with the minimum latency. With r_s as a control variable, we model $r_r = \mathcal{R}_r(r_s)$ as being chosen such that no regular vehicle could switch roads to experience a lower delay. If there are regular vehicles present on both roads, the delay on the roads must be equal. In this non-atomic model, where each operator controls an infinitesimally small unit of flow, if one of the roads had lower delay then a driver from the other road would switch to it. This would continue until the roads had equal latency or there are no regular vehicle drivers on the road with longer delay. Thus, both roads having equal delay is a Wardrop Equilibrium.

A Wardrop Equilibrium also exists if all regular vehicles are on one road ($r_r = 0$ or $r_r = 1$) and the other road, which has only autonomous vehicles, has a longer delay.

The first case in which roads have equal delay satisfies $D_1(r_r, r_s, C_1) = D_2(\overline{r}_r, \overline{r}_s, C_2)$. In the general case we denote the best-response mapping of regular vehicles to smart vehicle routing as $\mathcal{R}_r(r_s)$, where $\mathcal{R}_r : [0,1] \to [0,1]$. Given a r_s, finding r_r such that $D_1 = D_2$ involves finding the solution of a third order polynomial.

We are concerned with the cost at the worst-case Wardrop equilibrium, which we denote by

$$L(r_s, \mathcal{R}_r(r_s)) = \max_{\tilde{r}_r \in \mathcal{R}^{EQ}(r_s)} \{L(r_s, \tilde{r}_r)\},$$

where $\mathcal{R}^{EQ}(r_s)$ denotes the set of Nash Equilibria for control variable r_s, and has cardinality at most 3.

Noting that $\overline{\mathcal{R}}_r(r_s) = 1 - \mathcal{R}_r(r_s)$, the objective is to find

$$\begin{aligned} r_s^* &= \underset{r_s}{\operatorname{argmin}}\, L(r_s, \mathcal{R}_r(r_s)) \\ &= \underset{r_s}{\operatorname{argmin}}\Big(\frac{b\lambda_r \mathcal{R}_r(r_s) + a\lambda_s r_s}{ab - b\lambda_r \mathcal{R}_r(r_s) - a\lambda_s r_s} \\ &\quad + \frac{k(d\lambda_r \overline{\mathcal{R}}_r(r_s) + c\lambda_s \bar{r}_s)}{cd - d\lambda_r \overline{\mathcal{R}}_r(r_s) - c\lambda_s \bar{r}_s}\Big) \end{aligned} \tag{8}$$

To summarize, we aim to find the best control strategy for smart vehicles such that the social cost is minimized when regular vehicles choose their routes selfishly. While we have not fully characterized the solution of this optimization problem analytically, we later provide numerical simulations that suggest convexity of the optimization problem.

IV. Solution Description

In this section we develop solutions to the two optimization problems posed in Section III. We describe a closed-form solution for the social planner case and a numerical gradient descent algorithm for the selfish routing case.

A. Social Planner

As shown in Theorem 1, the solution to the social planner will lie on an extremity of the region of consideration. Using this we have developed a simple closed form solution for finding the optimal feasible social planner routing. To describe the solution, first we examine the four possible regions for the social optimal solution:

(i) The r_r axis, which has minimum at $r_s = 0$, $r_r = \frac{\sqrt{a}(-cd+d\lambda_r+c\lambda_s+\sqrt{ackd})}{(\sqrt{a}+\sqrt{ck})d\lambda_r}$

(ii) The r_s axis, which has minimum at $r_s = \frac{\sqrt{b}(-cd+d\lambda_r+c\lambda_s+\sqrt{bdkc})}{(\sqrt{b}+\sqrt{dk})c\lambda_s}$, $r_r = 0$

(iii) The $\bar{r}_r$ axis, which has minimum at $r_s = 1$, $r_r = \frac{\sqrt{a}(-bc+b\lambda_r-\sqrt{ack}\lambda_s+\sqrt{ack}b)}{(\sqrt{a}+\sqrt{ck})b\lambda_r}$

(iv) The $\bar{r}_s$ axis, which has minimum at $r_s = \frac{\sqrt{b}(-ad-\sqrt{bdk}\lambda_r+a\lambda_s+\sqrt{bdk}a)}{(\sqrt{b}+\sqrt{dk})a\lambda_s}$, $r_r = 1$

To find the global optimum, first we ensure that the intersection of the feasibility region and the region of consideration is nonempty. Then we do the following:

1) If the feasibility region opens left, meaning $\frac{a}{b} > \frac{c}{d}$:
   a) Check the r_r axis, as in (i). If $r_r \in [0,1]$, then this is the optimal solution. If $r_r < 0$, proceed to 1b. If $r_r > 1$, proceed to 1c.
   b) Check the r_s axis, as in (ii). If $r_s \in [0,1]$, then this is the optimal routing configuration. Otherwise, if $r_s < 0$, choose $(r_s^{OPT}, r_r^{OPT}) = (0,0)$.
   c) Check the $\bar{r}_s$ axis, as in (iv). If $r_s \in [0,1]$, then this is the optimal routing configuration. Otherwise, if $r_s < 0$, choose $(r_s^{OPT}, r_r^{OPT}) = (0,1)$, and if $r_s > 1$, choose $(r_s^{OPT}, r_r^{OPT}) = (1,1)$.
2) If the feasibility region opens right or the lines are parallel, meaning $\frac{a}{b} \le \frac{c}{d}$:
   a) Check the $\bar{r}_r$ axis, as in (iii). If $r_r \in [0,1]$, then this is the optimal solution. If $r_r < 0$, proceed to 2b. If $r_r > 1$, proceed to 2c.
   b) Check the r_s axis, as in (ii). If $r_s \in [0,1]$, then this is the optimal routing configuration. Otherwise, if $r_s < 0$, choose $(r_s^{OPT}, r_r^{OPT}) = (0,0)$, and if $r_s > 1$, choose $(r_s^{OPT}, r_r^{OPT}) = (1,0)$.
   c) Check the $\bar{r}_s$ axis, as in (iv). If $r_s \in [0,1]$, then this is the optimal routing configuration. Otherwise, if $r_s > 1$, choose $(r_s^{OPT}, r_r^{OPT}) = (1,1)$.

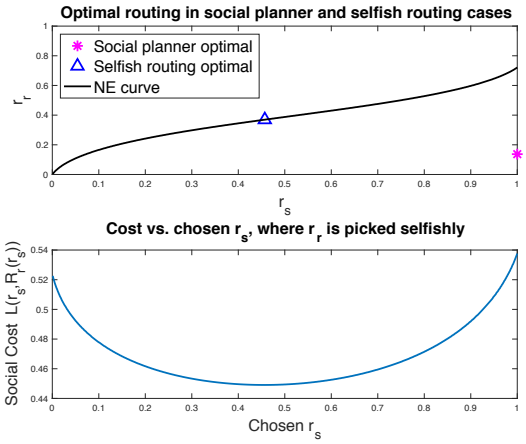

Fig. 4: Ex. 1: (a) Social optimal solution (magenta asterisk) and the selfish routing optimal solution (magenta triangle). (b) Aggregate delay as a function of r_s, where r_r is chosen selfishly. We observe convexity in this function, though we have not proven it analytically in the general case.

B. Selfish Routing

The function $r_r = \mathcal{R}_r(r_s)$ is the root of a third-order polynomial and does not lend itself to a closed-form solution. Instead we use a numerical gradient algorithm to find the minimum of $L(r_s, \mathcal{R}_r(r_s))$, shown in Fig. 4 (b). Though we have not proven convexity, numerical results show convexity for the region where the delays on each road are equal as well as the region where the delays on the roads are not equal. Because of this we use a gradient algorithm in each region to find the minima and then compare the two.

V. Numerical Results and Discussion

In this section we present three example scenarios with their optimal routings and costs (Table I). For all these examples, $k = 1$. In each, we compare the following three quantities, with $L_1 \le L_3 \le L_2$:

(i) the social optimum cost, $L_1 = L(r_s^{OPT}, r_r^{OPT})$,
(ii) the cost when r_s is chosen as the social planner optimal solution and r_r is chosen selfishly, $L_2 = L(r_s^{OPT}, \mathcal{R}_r(r_s^{OPT}))$, and,
(iii) the cost when r_s is chosen to optimize cost when r_r is chosen selfishly, $L_3 = L(r_s^*, \mathcal{R}_r(r_s^*))$.

In the first example there are two roads with similar capacity, each with about three times the smart capacity as regular capacity. In Fig. 4 (a) we see that the social optimal solution appears on the $\bar{r}_r$ axis and the optimal Wardrop solution appears in the interior of the feasibility region.

The three examples represent different regimes: in each successive example the relative benefit of choosing r_s^* instead of r_s^{OPT} decreases until, in the third example, $r_s^* = r_s^{OPT}$ and $L_2 = L_3$.

TABLE I: Results

	Ex. 1	Ex. 2	Ex. 3
a	10	10	50
b	30	30	60
c	12	25	60
d	32	32	160
λ_r	3	8	30
λ_s	3	15	100
r_s^{OPT}	1.0	0.78	0
r_r^{OPT}	0.14	0	0.97
L_1	0.439	1.385	3.22
r_s^{OPT}	1.0	0.78	0
$\mathcal{R}_r(r_s^{OPT})$	0.72	0.05	0.66
L_2	0.537	1.441	4.44
r_s^*	0.47	0.87	0
$\mathcal{R}_r(r_s^*)$	0.37	0	0.66
L_3	0.449	1.402	4.44

Table I: Results for three routing scenarios. Three quantities are compared: (i) the optimal cost, L_1, when both regular and smart cars are routed by a social planner, (ii) the cost, L_2, when regular cars selfishly route and smart cars are routed as in (i), and (iii) the optimal cost, L_3, when smart cars are routed by a social planner and regular cars choose selfishly.

VI. CONCLUSIONS

In this paper we have presented two models for road capacity under mixed autonomy and described a specific case with two parallel roads. We modeled cases in which a planner has control over both regular and smart traffic flows and the case that regular vehicles route selfishly in response to the routing choices of the smart vehicles. We have developed a geometric interpretation of the cost function under capacity model 1 to prove convexity and provided a closed-form solution for the social planner case. We provide numerical results that indicate convexity in the selfish-routing case and exemplify performance in different scenarios.

REFERENCES

[1] G. Orosz, "Connected cruise control: modelling, delay effects, and nonlinear behaviour," *Vehicle System Dynamics*, pp. 1–30, 2016.

[2] R. Pueboobpaphan and B. van Arem, "Driver and vehicle characteristics and platoon and traffic flow stability: Understanding the relationship for design and assessment of cooperative adaptive cruise control," *Transportation Research Record: Journal of the Transportation Research Board*, no. 2189, pp. 89–97, 2010.

[3] J. Lioris, R. Pedarsani, F. Y. Tascikaraoglu, and P. Varaiya, "Platoons of connected vehicles can double throughput in urban roads," *arXiv preprint arXiv:1511.00775*, 2015.

[4] S. E. Shladover, "Longitudinal control of automated guideway transit vehicles within platoons," *Journal of Dynamic Systems, Measurement, and Control*, vol. 100, no. 4, pp. 302–310, 1978.

[5] S. Darbha and K. Rajagopal, "Intelligent cruise control systems and traffic flow stability," *Transportation Research Part C: Emerging Technologies*, vol. 7, no. 6, pp. 329–352, 1999.

[6] J. Yi and R. Horowitz, "Macroscopic traffic flow propagation stability for adaptive cruise controlled vehicles," *Transportation Research Part C: Emerging Technologies*, vol. 14, no. 2, pp. 81–95, 2006.

[7] J. Vander Werf, S. Shladover, M. Miller, and N. Kourjanskaia, "Effects of adaptive cruise control systems on highway traffic flow capacity," *Transportation Research Record: Journal of the Transportation Research Board*, no. 1800, pp. 78–84, 2002.

[8] B. Van Arem, C. J. Van Driel, and R. Visser, "The impact of cooperative adaptive cruise control on traffic-flow characteristics," *IEEE Transactions on Intelligent Transportation Systems*, vol. 7, no. 4, pp. 429–436, 2006.

[9] R. Jiang, M.-B. Hu, B. Jia, R. Wang, and Q.-S. Wu, "Phase transition in a mixture of adaptive cruise control vehicles and manual vehicles," *The European Physical Journal B*, vol. 58, no. 2, pp. 197–206, 2007.

[10] Y.-M. Yuan, R. Jiang, M.-B. Hu, Q.-S. Wu, and R. Wang, "Traffic flow characteristics in a mixed traffic system consisting of ACC vehicles and manual vehicles: A hybrid modelling approach," *Physica A: Statistical Mechanics and its Applications*, vol. 388, no. 12, pp. 2483–2491, 2009.

[11] A. Kesting, M. Treiber, and D. Helbing, "Enhanced intelligent driver model to access the impact of driving strategies on traffic capacity," *Philosophical Transactions of the Royal Society of London A: Mathematical, Physical and Engineering Sciences*, vol. 368, no. 1928, pp. 4585–4605, 2010.

[12] G. M. Arnaout and S. Bowling, "A progressive deployment strategy for cooperative adaptive cruise control to improve traffic dynamics," *International Journal of Automation and Computing*, vol. 11, no. 1, pp. 10–18, 2014.

[13] J. Lee and B. Park, "Development and evaluation of a cooperative vehicle intersection control algorithm under the connected vehicles environment," *IEEE Transactions on Intelligent Transportation Systems*, vol. 13, no. 1, pp. 81–90, 2012.

[14] E. Dallal, A. Colombo, D. Del Vecchio, and S. Lafortune, "Supervisory control for collision avoidance in vehicular networks with imperfect measurements," in *2013 IEEE 52nd Annual Conference on Decision and Control (CDC)*, pp. 6298–6303, IEEE, 2013.

[15] D. Miculescu and S. Karaman, "Polling-systems-based control of high-performance provably-safe autonomous intersections," in *53rd IEEE Conference on Decision and Control*, pp. 1417–1423, IEEE, 2014.

[16] A. Colombo and D. Del Vecchio, "Least restrictive supervisors for intersection collision avoidance: A scheduling approach," *IEEE Transactions on Automatic Control*, vol. 60, no. 6, pp. 1515–1527, 2015.

[17] P. Tallapragada and J. Cortés, "Coordinated intersection traffic management," *IFAC-PapersOnLine*, vol. 48, no. 22, pp. 233–239, 2015.

[18] Y. J. Zhang, A. A. Malikopoulos, and C. G. Cassandras, "Optimal control and coordination of connected and automated vehicles at urban traffic intersections," in *2016 American Control Conference (ACC)*, pp. 6227–6232, July 2016.

[19] A. Askari, D. A. Farias, A. A. Kurzhanskiy, and P. Varaiya, "Measuring impact of adaptive and cooperative adaptive cruise control on throughput of signalized intersections," *arXiv preprint arXiv:1611.08973*, 2016.

[20] J. Wardrop, "Some theoretical aspects of road traffic research," in *Inst Civil Engineers Proc London/UK/*, 1900.

[21] A. Charnes and W. Cooper, "Multicopy traffic network models," *Theory of traffic flow*, vol. 85, pp. 85–96, 1961.

[22] S. C. Dafermos and F. T. Sparrow, "The traffic assignment problem for a general network," *Journal of Research of the National Bureau of Standards B*, vol. 73, no. 2, pp. 91–118, 1969.

[23] A. Haurie and P. Marcotte, "On the relationship between Nash—Cournot and Wardrop equilibria," *Networks*, vol. 15, no. 3, pp. 295–308, 1985.

[24] E. Koutsoupias and C. Papadimitriou, "Worst-case equilibria," in *Annual Symposium on Theoretical Aspects of Computer Science*, pp. 404–413, Springer, 1999.

[25] C. Papadimitriou, "Algorithms, games, and the internet," in *Proceedings of the thirty-third annual ACM symposium on Theory of computing*, pp. 749–753, ACM, 2001.

[26] T. Roughgarden and É. Tardos, "How bad is selfish routing?," *Journal of the ACM (JACM)*, vol. 49, no. 2, pp. 236–259, 2002.

[27] T. Roughgarden, "The price of anarchy is independent of the network topology," *Journal of Computer and System Sciences*, vol. 67, no. 2, pp. 341–364, 2003.

[28] J. R. Correa, A. S. Schulz, and N. E. Stier-Moses, "Selfish routing in capacitated networks," *Mathematics of Operations Research*, vol. 29, no. 4, pp. 961–976, 2004.

[29] C. K. Chau and K. M. Sim, "The price of anarchy for non-atomic congestion games with symmetric cost maps and elastic demands," *Operations Research Letters*, vol. 31, no. 5, pp. 327–334, 2003.

[30] G. Perakis, "The "price of anarchy" under nonlinear and asymmetric costs," *Mathematics of Operations Research*, vol. 32, no. 3, pp. 614–628, 2007.

[31] Transportation Research Board, "Highway capacity manual," 2000.

[32] V. Milanés, S. E. Shladover, J. Spring, C. Nowakowski, H. Kawazoe, and M. Nakamura, "Cooperative adaptive cruise control in real traffic situations," *IEEE Transactions on Intelligent Transportation Systems*, vol. 15, no. 1, pp. 296–305, 2014.

[33] The Economist, "A breakthrough in miniaturising lidars for autonomous driving," *The Economist*, December 24, 2016.